



Actinide targets for the synthesis of superheavy nuclei

J. B. Roberto^a, M. Du, J. G. Ezold, S. L. Hogle[✉], J. Moon, K. Myhre, K. P. Rykaczewski

Oak Ridge National Laboratory, Oak Ridge, TN 37831, USA

Received: 2 May 2023 / Accepted: 28 September 2023 / Published online: 26 December 2023

© UT-Battelle, LLC 2023

Communicated by Klaus Blaum

Abstract The use of heavy actinide targets, including ^{243}Am , $^{240,242,244}\text{Pu}$, $^{245,248}\text{Cm}$, ^{249}Bk , and ^{249}Cf , irradiated by intense heavy ion beams of ^{48}Ca has resulted in a significant expansion of the periodic table since 2000, including the discovery of five new heaviest elements and more than 50 new isotopes. These actinide materials can only be produced by intense neutron irradiation in very high flux reactors followed by chemical processing and purification in specialized hot cell facilities available in only a few locations worldwide. This paper reviews the reactor production of heavy actinides, the recovery and chemical separation of actinide materials, and the preparation of actinide targets for superheavy element experiments. The focus is on ^{248}Cm , ^{249}Bk , mixed $^{249-251}\text{Cf}$, and ^{254}Es , including current availabilities and new production processes. The impacts of new facilities, including the Superheavy Element Factory at Dubna, accelerator and separator upgrades at RIKEN, and proposed upgrades to the High Flux Isotope Reactor at Oak Ridge are also described. Examples of recent superheavy element research are discussed as well as future opportunities for superheavy research using actinide targets.

1 Introduction

The use of actinide targets in combination with intense heavy ion beam irradiation has transformed superheavy element (SHE) research, significantly expanding the periodic table by adding five new heaviest elements since 2012 [1–3]. These advances have been accomplished using the “hot fusion” technique [4], where heavy actinide targets, typically ^{243}Am , $^{240,242,244}\text{Pu}$, $^{245,248}\text{Cm}$, ^{249}Bk , and ^{249}Cf , are bombarded with ^{48}Ca beams at large accelerator facilities, creating compound nuclei that decay to superheavy nuclei with half-lives ranging up to many hours for lower proton numbers (Z) to

hundreds of microseconds for higher Z s. Heavy actinides can only be produced in the required quantities (i.e., tens of milligrams) using very high flux reactors and large-scale radiochemical processing facilities available at only a few research institutions worldwide [5]. The most recent five elements, flerovium, moscovium, livermorium, tennessine, and oganesson, with $Z = 114–118$, were discovered using actinides from the High Flux Isotope Reactor (HFIR) and adjacent Radiochemical Engineering Development Center (REDC) at Oak Ridge National Laboratory (ORNL) and the SM-3 Reactor at the Research Institute of Advanced Reactors (RIAR) in Dmitrovgrad, Russia. These elements were originally produced [6–9] using the U400 cyclotron at the Flerov Laboratory at the Joint Institute for Nuclear Research (JINR) in Dubna, Russia, with later confirmations at accelerator facilities at Lawrence Berkeley National Laboratory (LBNL) [10, 11]; the Gesellschaft für Schwerionenforschung (GSI), Darmstadt, Germany [12–15], and JINR [16]. Most actinide materials for current SHE experiments have been produced and/or processed at HFIR/REDC through the US Department of Energy (DOE) Isotope Program.

Actinides are radioactive elements with atomic numbers $Z = 89–103$. They were first described as a new row in the periodic table by Seaborg [17] in the 1940s. Accumulating more than trace amounts of actinides heavier than uranium requires production in nuclear reactors. Heavy actinides are the highest Z target materials available, making them attractive for the synthesis of SHEs (i.e., elements with atomic numbers of 104 or greater). For a given superheavy element, higher Z targets and the neutron-rich ^{48}Ca projectile lead to more asymmetric nuclear reactions with correspondingly lower Coulomb barriers in comparison to the cold fusion reactions with ^{208}Pb and ^{209}Bi targets and beams heavier than ^{48}Ca . Heavy actinides also have higher neutron numbers, and ^{48}Ca projectiles provide additional excess neutrons. This results in compound nuclei closer to the shell closure at $N = 184$ with corresponding increases in survivability

^a e-mail: robertojb@ornl.gov (corresponding author)

against fission further increasing production cross sections for neutron-rich nuclei. Cold fusion techniques led to the discovery of elements 107–113 [18–24], but production rates steadily declined with increasing Z to below one atom per year for element 113 [24], making further progress impractical. The path of hot fusion with actinide targets and ^{48}Ca beams increased production rates by factors of 10 and more [25], enabling expansion of the periodic table beyond $Z = 113$ to $Z = 118$. Ongoing and proposed SHE searches for new elements 119 at RIKEN [26] and 120 at JINR [27] and LBNL [28] are also dependent on actinide targets.

In this paper, we review the production, processing, and applications of heavy actinide materials for SHE research and discovery. This includes actinide production in reactors, recovery of actinides from reactor-irradiated materials, chemical processing and purification of actinides, and target preparation and performance. The focus is on ^{248}Cm , ^{249}Bk , mixed $^{249-251}\text{Cf}$, and ^{254}Es , including current availabilities and new production processes. The impacts of new facilities, including the Superheavy Element Factory at JINR [29], accelerator upgrades at RIKEN [26], new facilities under construction at GANIL [30] and GSI [31, 32], and proposed upgrades to HFIR [33] are also discussed. We also review the status of some current experiments and discuss future opportunities for superheavy research using heavy actinide targets. In addition to new element discovery, these opportunities include nuclear structure studies [34], atomic physics [35], mass number measurements [11], mass measurements [36, 37], and chemistry studies [38] for superheavy nuclei and atoms, but these are not in the focus of this article.

2 Production and availability of actinides

ORNL is the major global supplier of heavy actinides, including ^{252}Cf , ^{249}Bk , and ^{254}Es . The SM-3 reactor in Russia also contributes to global ^{252}Cf supplies. ORNL has unique facilities for the production and processing of heavy actinides, including HFIR and REDC, and has decades of experience synthesizing, separating, purifying, and transporting transuranium radioisotopes [39–41]. These ORNL-produced materials play a key role in advancing scientific understanding of both heavy element chemistry (HEC) and fundamental nuclear structure.

ORNL has provided actinide target materials that have been used for the synthesis of all SHEs above element 112 [6–9, 42], and in some cases has carried out fabrication of the experimental targets [27]. These experiments have been performed at JINR and GSI in collaboration with US laboratories including ORNL. Future discoveries of elements 119 and 120 will require heavier ion beams, and/or heavier target materials, than those used in earlier experiments. Further, the reactions resulting in synthesis of these heavier

isotopes are expected to have significantly lower probabilities [43–45] than those of earlier work. This in turn requires larger quantities of materials, and targets capable of sustaining a longer beam time, to observe the same number of reactions. Larger quantities of produced target materials can support thicker targets [46] to increase yields using separators with high acceptance angles, allow for increased target damage and material losses associated with higher beam currents and doses, and compensate for decay losses for experiments involving short-lived targets such as ^{249}Bk .

ORNL further provides actinide materials in support of basic research on the fundamental chemistry of actinide elements. Current electronic structure methods are unable to accurately describe the behavior of f -electrons, such as spin–orbit coupling, multiplet complexity, and relativistic effects. Synthetic chemistry, spectroscopy, and structural characterization explore the chemical and physical properties of these elements to determine their bonding and reactivity in solution, at the interface, and in the solid state. Increased supply of heavy actinides increases the number and complexity of experiments that can be performed on the materials and accelerates the rate of progress in Heavy Element Chemistry [25, 46–48].

2.1 ORNL's Californium-252 Program

The Californium-252 Program is the second largest isotope production program at ORNL, next to the Plutonium-238 Supply Program, and the largest program at ORNL that is managed through the DOE Isotope Program. ORNL has been producing ^{252}Cf for nearly 60 years and to date has supplied approximately 1.2 g of ^{249}Bk , 10.2 g of ^{252}Cf , 39 mg ^{253}Es , and 15 pg of ^{257}Fm from 79 campaigns.

These transcurium isotopes are produced by irradiation of targets composed of mixed Pu, Am, and Cm at HFIR, where they are exposed to one of the highest steady-state neutron fluxes in the world. The feed material is transmuted into heavier isotopes by a series of neutron captures and beta decays as shown in Fig. 1.

Transcurium isotopes are currently produced at ORNL on a regular 2-year schedule. The process begins with conversion of the actinide source material to oxide microspheres that are blended with aluminum powder and pressed to form cermet pellets. As shown in Fig. 2, these pellets are loaded into long, thin, finned aluminum tubes (i.e., targets) that are closure welded and then hydrostatically compressed to provide adequate heat transfer between the pellets and target tubes. A final aluminum jacket is wrapped around the target tube to channel the coolant flow around the target during irradiation (Fig. 2). The amount of actinide material in each target is limited both in mass, to reduce heat generation, and volume, to maintain heat transfer through the aluminum matrix and allow for containment of fission gasses.

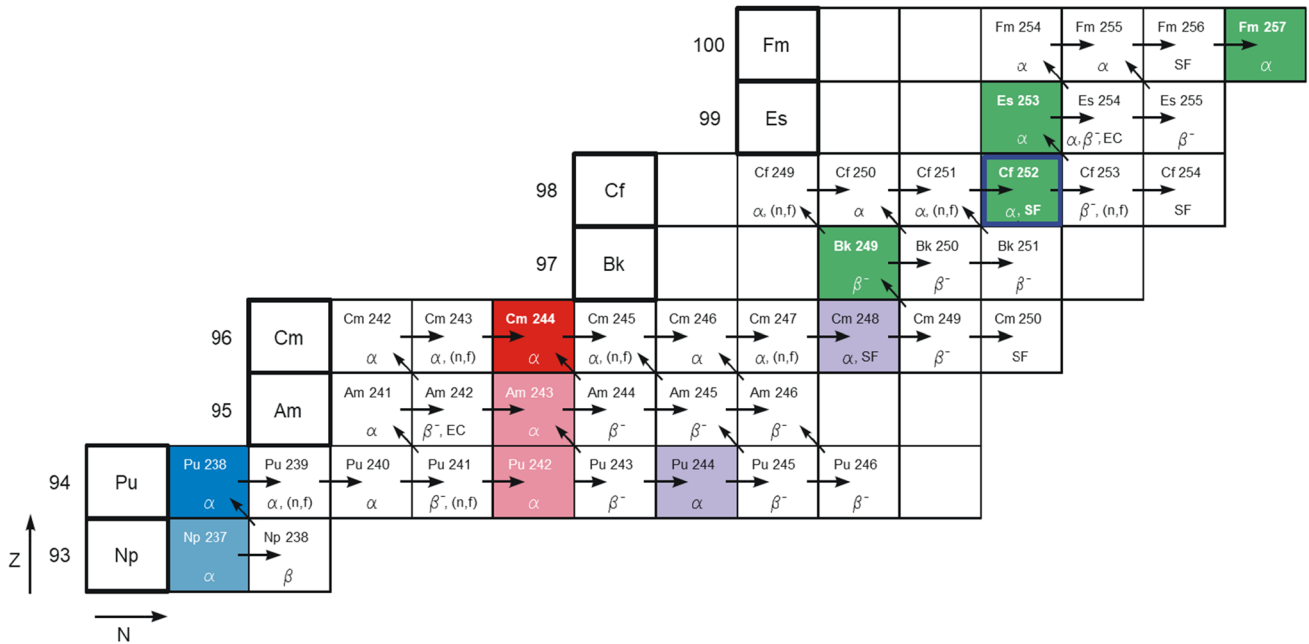


Fig. 1 Production of heavy actinides isotopes requires multiple neutron captures in a very high flux reactor

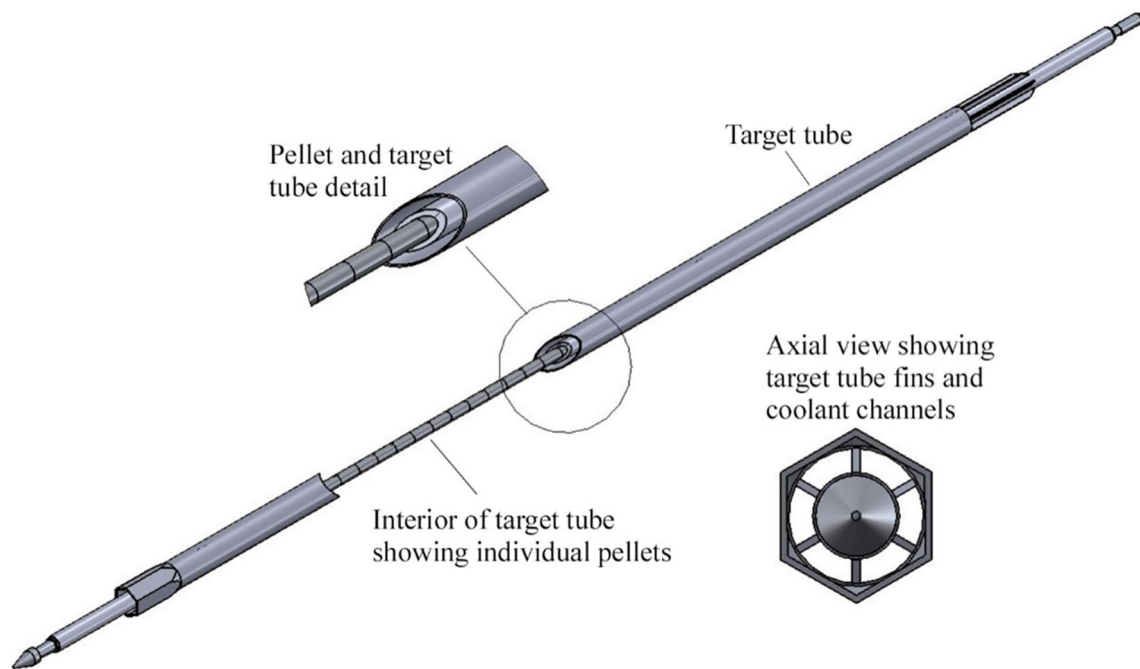


Fig. 2 Californium production target. The total length of the target rod is 36 inches with each pellet being 0.606 inches long with a 0.25 inch diameter

Following irradiation, the targets cool in the HFIR storage pool for approximately 2–3 months for decay of fission and activation products, particularly ^{131}I , a highly dispersible and radiotoxic fission product. The targets are then transferred to REDC for separation and purification of transcurium actinides. The chemical processing of neutron-irradiated targets to recover Cf and Bk is illustrated in Fig. 3.

The aluminum components are dissolved in a sodium hydroxide (NaOH) and sodium nitrate (NaNO_3) mixture [49] and heated, which results in dissolved aluminum as $\text{Al}(\text{OH})_4^-$ and precipitated metal hydroxides. The actinide and lanthanide solids are filtered and washed several times and then dissolved in HNO_3 . After dissolution, the desired

was configured to operate in a very-high-flux mode, and > 8 kg of ^{242}Pu contained in 86 Mk-18A targets were irradiated to produce ^{252}Cf for use in neutron source market development activities [55]. Twenty-one of these targets were processed at ORNL in the early 1970s to recover the ^{252}Cf , heavy curium (i.e., curium rich in $^{246-248}\text{Cm}$ isotopes), and ^{244}Pu . The remaining 65 Mk-18A irradiated targets contain the unique supply of heavy curium, which is likely to never to be produced again; the targets are currently in wet storage at the SRS [56]. These materials will be processed to recover the heavy curium [57, 58].

The targets will be retrieved from wet storage at SRS and transferred to shielded cells at Savannah River National Laboratory where they will be processed to recover an americium-curium-lanthanide product from the targets. The recovered materials will then be packaged and shipped to ORNL for storage, processing, and future distribution to end users. This will preserve the world's supply of irreplaceable heavy curium, as well as provide the DOE Isotope Program with feedstock for heavy isotope production. The Mk-18A materials will provide sufficient curium feedstock to produce ^{252}Cf and other heavy elements for the next several decades.

2.4 Long-lived actinides

The longer-lived lighter actinide target materials with atomic numbers below $Z = 97$, including $^{244,245,248}\text{Cm}$, $^{241,243}\text{Am}$, $^{240,242,244}\text{Pu}$, ^{238}U , ^{237}Np , and ^{232}Th are used in SHE research that involves connecting the “island of stability”¹ to the nuclear mainland, to study ground-state fission, alpha emission probabilities, and the structure of ground and excited states.

These target materials can also be used to investigate reaction mechanisms using increasingly available high intensity beams such as ^{48}Ca , ^{50}Ti , ^{51}V , and ^{54}Cr . The heaviest among these isotopes, $Z = 96$ ^{248}Cm , is presently used in a search for $Z = 119$ (using a ^{51}V beam at RIKEN) and can be used for a new element $Z = 120$ synthesis (using a ^{54}Cr beam). Experiments using curium, americium, plutonium, and neptunium isotopes, with moderately high cross sections at the level of 1 to 10 picobarn with ^{48}Ca beams are suitable—based on their scientific importance or actual efficiency of the experiments—for beam times of several months to years. The demand for these isotopes is expected to be approximately 15 to 100 mg per target. The lighter actinides, thorium, uranium, americium, radium, and $^{243-244}\text{Cm}$ can also be used for reaction and spectroscopy studies.

¹ The island of stability is a predicted region at the upper limits of the periodic table where shell closures in the vicinity of $Z = 114$ (or perhaps 120 or 124) and $N = 184$ are expected to confer increased stability on superheavy nuclei [59–62], resulting in long lifetimes for nuclei in this region.

ORNL maintains a legacy inventory of these long-lived isotopes in inventory and purifies and dispenses in the desired form for use in SHE and other research.

2.4.1 Long-lived ^{248}Cm recovery from decayed ^{252}Cf

Particularly important for SHE research is the long-lived heavy isotope ^{248}Cm ($T_{1/2} = 348,000$ years), only one proton below ^{249}Bk . Used for research similar to lighter elements neptunium through americium, the chemical properties of curium make it a very robust target, proven to survive long irradiations with heavy ion beams including doses in excess of 10^{19}cm^2 for ^{48}Ca [26, 63]. Long half-life and relatively low radioactivity make high-weight-percent ^{248}Cm a target of choice for many laboratories. A discovery campaign for element 119 is currently underway at RIKEN using ORNL-supplied ^{248}Cm and ^{51}V beams, with additional material required to supplement this target in the coming years. Following an upgrade to the ^{54}Cr beam, a discovery campaign for element 120 can be run with ^{248}Cm target material. This reaction was already tried for the element 120 synthesis at GSI in collaboration with ORNL and the University of Tennessee, Knoxville, resulting in an upper limit single event cross section of $0.58 (+ 1.34, - 0.48)$ pb [64] for this reaction. Upper limits for element 120 synthesis of 0.4 pb for the $^{244}\text{Pu} + ^{58}\text{Fe}$ reaction [65] and of 0.065 pb for the $^{249}\text{Bk} + ^{50}\text{Ti}$ reaction [66] have also been established. In addition to its importance as a target for SHE research, ^{248}Cm is the starting point for production of the heavier transcurium isotopes that are also used in SHE research.

During the initial processing and recovery of ^{252}Cf from irradiated targets, Cf storage packages are prepared. As the material is processed for source preparation and dispensing, individual storage packages are stripped with nitric acid to recover the Cf isotopes for further purification and program use, leaving behind ^{248}Cm in the range of 95–96 wt%, with some residual ^{252}Cf [67].

Another source of decay-produced ^{248}Cm is from 20- to 30-year decayed ^{252}Cf sources, which also generate high wt% ^{251}Cf with trace amounts of ^{252}Cf depending upon the age of the source. This level of ^{248}Cm enrichment is low for SHE target material but may be useful for the production of ^{249}Bk or other transcurium isotopes. The process of harvesting decayed ^{252}Cf sources is presented in more detail in the discussion concerning the recovery of ^{251}Cf in Sect. 2.4.2.

2.4.2 Long-lived mixed californium isotopes following ^{252}Cf decay

Since the beginning of operations at the REDC in 1966, 79 campaigns have been completed to produce the transcurium actinides, with ^{252}Cf being the isotope produced in the highest quantity. During production of ^{252}Cf , the other

Table 1 Typical Cf product isotopic distribution from HFIR irradiation

Isotope	At %	$T_{1/2}$, y
^{249}Cf	3.4	351
^{250}Cf	8.7	13.1
^{251}Cf	2.6	898
^{252}Cf	85.3	2.65

californium isotopes (i.e., ^{249}Cf , ^{250}Cf , ^{251}Cf), and shorter-lived ^{253}Cf are also produced. A typical distribution for the Cf product is shown in Table 1 with the corresponding half-life for each isotope.

The ^{252}Cf sources were provided to various DOE national laboratories, other government agencies, and universities for research. When a facility no longer needed the sources or needed a replacement source of higher strength, the decayed source was returned to ORNL and placed in the storage pool for potential future use. Many of these sources have been in the storage pool for decades, resulting in decay-enriched material that contains the longer-lived californium isotopes. This unique target material has been recovered twice in recent history for use in mixed californium sources [68]. Recovery involves the following steps:

1. Sources are retrieved from the storage pool and cut open in a shielded hot cell (Fig. 4).
2. The aluminum pellets are dissolved out of the source in a solution of NaOH and NaNO₃, leaving behind the stainless-steel capsule and the solid, black californium and curium (Fig. 5).
3. The solid californium and curium are dissolved in HNO₃ and processed through several cleanup columns (DGA, LN, TEVA, MP-1) and concentrator columns to remove other actinides and contaminants from the californium fraction.

2.5 Short-lived ^{249}Bk

Berkelium-249, with a half-life of 327 days, is a radioisotope of interest in the nuclear physics and chemistry communities as a target for production of the most neutron-rich and longer-lived isotopes of superheavy elements. In addition to nuclear structure studies, the isotopes produced in the decay chains of $Z = 117$ isotopes have half-lives long enough to conduct studies of their chemical properties.

Berkelium is currently produced as a byproduct of the Californium-252 Program. Yields of ^{249}Bk are not proportional to yields of ^{252}Cf , but rather are proportional to the total amount of irradiated ^{248}Cm in the batch of ^{252}Cf production targets. Californium production campaigns operate



Fig. 4 Buehler IsoMet™ Low Speed Precision Cutter sawing the outer stainless-steel capsule of a californium source

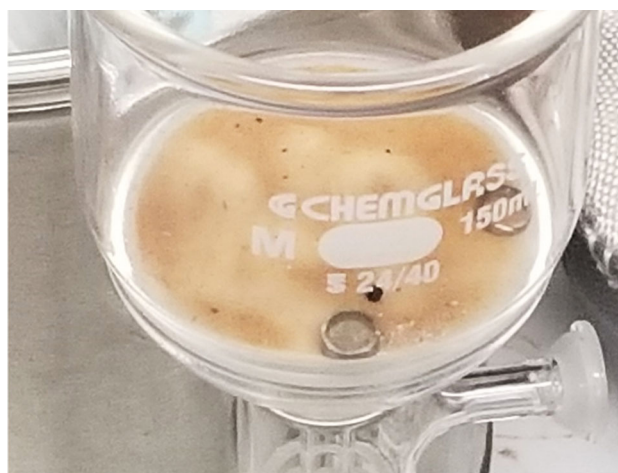


Fig. 5 Stainless-steel capsule (metal rings) and black pellet of californium and curium remaining after filtration of the dissolved solution

on a regular 2-year schedule and typically produce 10–15 mg of ^{249}Bk . The historical process of purifying ^{249}Bk is described in Sect. 2.2.

2.5.1 Ongoing research and development for production of ^{249}Bk

Current research aims to establish capabilities for production of ^{249}Bk from high-weight-percent curium feedstock and evaluate the use of thermal neutron filters to reduce the burnup rate of ^{249}Bk in reactor, increasing the saturation activity [39–41]. A diagram of the target to be used for this irradiation is shown in Fig. 6; the target employs a 1.6 mm natural gadolinium sleeve inside a large bore aluminum capsule. Inside the gadolinium sleeve is a curium oxide and aluminum cermet pellet. The gadolinium serves as the thermal neutron

Fig. 6 Berkelium-249 production target showing Cm pellet (yellow) inside a natural Gd sleeve (blue)

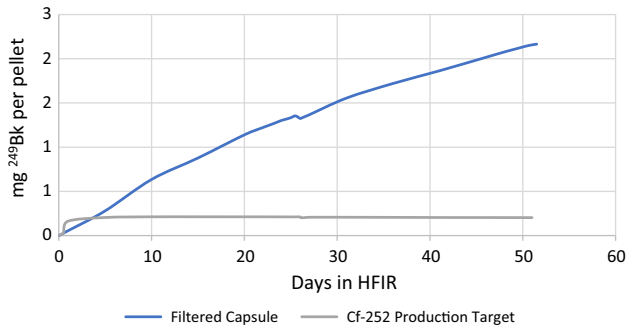
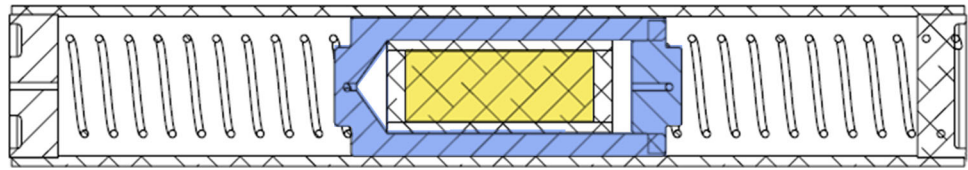


Fig. 7 Berkelium-249 production per pellet in filtered capsules vs. ²⁵²Cf production targets

filter, which reduces the effective flux of neutrons at energies that burn up the ²⁴⁹Bk at a higher rate than those inducing the desired ²⁴⁸Cm transmutation.

Modeling and simulation of this target design has predicted that 35 mg of ²⁴⁸Cm irradiated for one cycle will produce 1.0 mg of ²⁴⁹Bk and 0.1 mg of fission products, with ²⁴⁸Cm transmutation losses of 5%. Irradiation for two cycles will produce 1.6 mg of ²⁴⁹Bk and 0.3 mg of fission products, with ²⁴⁸Cm transmutation losses of 9%. Irradiation beyond two cycles will likely significantly deplete the Gd sleeve, resulting in loss of ²⁴⁹Bk due to thermal neutron absorption. The projected yield curves for ²⁴⁹Bk for this target, vs. for a pellet in a ²⁵²Cf production target, are shown in Fig. 7.

In addition to increased ²⁴⁹Bk yields, the gadolinium filter reduces the production of ²⁵²Cf by over 90% such that the irradiated material does not require heavy neutron shielding.

2.5.2 Ongoing research and development for purification of ²⁴⁹Bk

A dual-column separation procedure has recently been developed to replace the cation exchange (CX) -AHIB purification of ²⁴⁹Bk. The new technique is based on the discovery of a specific feature of Bk(IV) ions [69]: *Unlike any other tetravalent actinides, Bk(IV) does not form anion in high HNO₃ and is not adsorbed by anion exchange (AX) resin in high HNO₃ media.* The HNO₃ concentration here can be higher than 10 M [69]. This feature allows Bk(IV) to pass through an AX column with no adsorption while any other tetravalent actinides/impurity metals are adsorbed by the AX column. With the knowledge of Bk(IV) being adsorbed by

Eichrom LN resin (impregnated with HDEHP), a dual column of MP-1 and LN resins is designed as shown in Fig. 8, where a MP-1 resin column is installed on top of a LN resin column, both preconditioned with HNO₃ and NaBrO₃.

Bk(III) is oxidized to Bk(IV) by NaBrO₃, along with some radioactive impurities such as ^{141,144}Ce(III). Tetravalent metal ions are adsorbed by MP-1 column while ²⁴⁹Bk(IV) and mono-, di-, trivalent metal impurities (including iron) pass through the MP-1 column to the lower LN column. Bk(IV) is adsorbed by the LN column while mono-, di-, trivalent metal impurities (including iron) pass through the LN column into the waste collection bottle. The LN resin column is then detached from the stacked dual column and the purified ²⁴⁹Bk is stripped. This strip solution can be easily evaporated and adjusted to customer-required specifications [69].

Compared to the CX-AHIB process, dual-column operations are faster and require less expertise to execute. The process requires less scrubbing and evaporation, saving several days of process time. There are no high-temperature requirements and no drop counts for a chromatographic separation of impurities before or after the Bk fraction. Based on recent developmental work, the dual-column Bk recovery process results in a purified ²⁴⁹Bk fraction containing < 1 ng of ²⁵²Cf, with a 10⁷ or greater decontamination factor for all radionuclides.

2.6 Short-lived ²⁵⁴Es produced via irradiation

Einsteinium-254, with a half-life of 276 days, is another radioisotope of interest in the nuclear physics and chemistry communities. At 5 atomic mass units heavier than ²⁴⁹Bk, ²⁵⁴Es is capable of producing even heavier neutron-rich isotopes of SHEs. However, as there is no quasi-stable precursor to ²⁵⁴Es, as ²⁴⁸Cm is to ²⁴⁹Bk, production quantities are extremely small from multiple neutron-capture chains on heavy curium.

Einsteinium-254 is currently produced as a byproduct of the Californium-252 Program, similar to ²⁴⁹Bk, with approximately 1 μg available from every biennial ²⁵²Cf campaign. These quantities have been used for radiochemical determination of cross sections for the heaviest actinides produced in transfer reactions of ^{16,18}O and ²²Ne with an ²⁵⁴Es target [70], but are three orders of magnitude less than typically required for SHE production targets. ²⁵⁴Es material produced and separated at ORNL was recently used for the

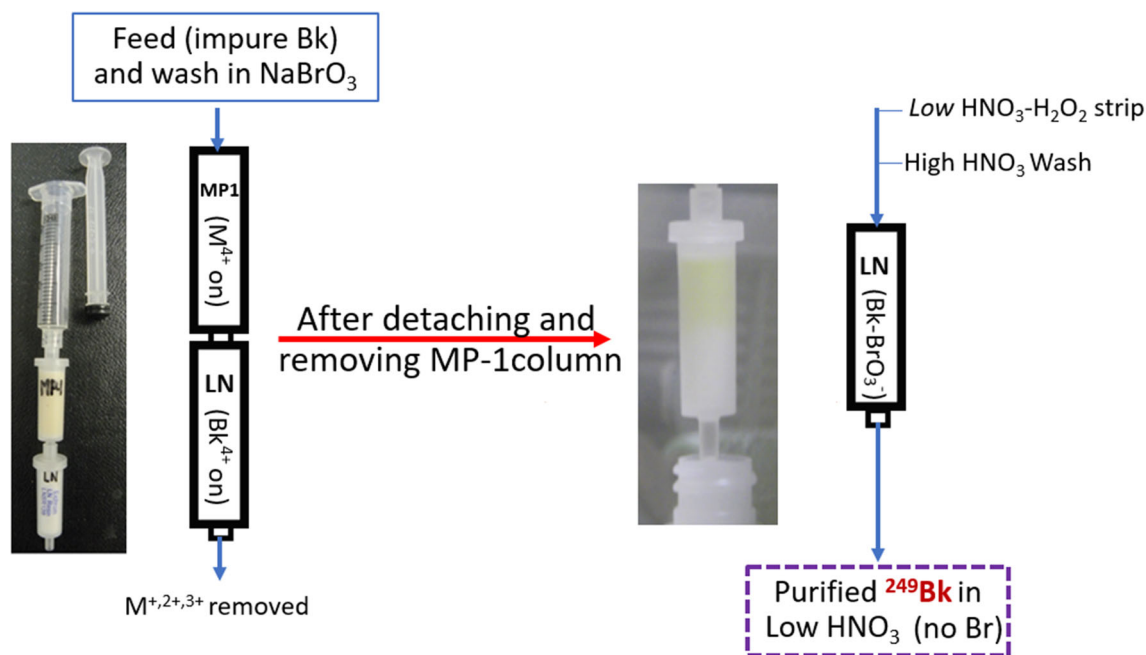


Fig. 8 Example of a dual-column (MP-1 /LN) separation procedure for treatment of solution of ≤ 15 mg ^{249}Bk -impurities

studies of the fission mechanism of ^{258}Md produced in $^4\text{He} + ^{254}\text{Es}$ reactions at the JAEA tandem accelerator facility and spontaneous fission of Fm isotopes at JAEA-ISOL. Fission studies using multinucleon transfer reactions of $^{18}\text{O} + ^{254}\text{Es}$ have also been carried out at JAEA [71].

Einsteinium fractions are obtained from the hot cell AHIB–cation exchange and transferred to a glove box. Product finishing consists of a cation cleanup column, TEVA column with thiocyanate, several iterations of AHIB separation, and a final cation column for AHIB removal.

2.6.1 Ongoing research and development for production of ^{254}Es

Current research aims to establish capabilities for production of ^{254}Es from high-weight-percent curium feedstock and evaluate the use of interchangeable external neutron filters to reduce the burnup rate of ^{254}Es in reactor, increasing the saturation activity. This work differs from the target design for ^{249}Bk production, in that ^{254}Es production first requires buildup of ^{253}Es and ^{253}Cf through capture of thermal neutrons. Therefore, a thermal neutron filter embedded in the sealed capsule would be ineffective. This research aims to develop a filter that can be located externally to the sealed capsule, being exposed to the HFIR cooling water. This would both allow for removal and replacement of the filter during HFIR maintenance outages and would provide improved heat removal for the highly neutron absorbing material. This work is still in early development but is expected to increase ^{254}Es production per unit ^{248}Cm by

roughly 500%, without a commensurate increase in ^{253}Es . The amount of Es that can be shipped to customers in a Type A package is and will be limited by the ^{253}Es activity.

2.7 Short-lived ^{257}Fm produced via neutron irradiation

Fermium-257, with a half-life of 100.5 days, is the heaviest isotope that can feasibly be produced in the HFIR. Fermium is currently produced as a byproduct of the Californium-252 Program, similarly to ^{249}Bk and ^{254}Es , with 0.5–1.0 pg of ^{257}Fm typically available per biennial campaign. Ongoing research and development aimed at increasing yields of ^{249}Bk and ^{254}Es will not produce increased yields of ^{257}Fm . Such an effort would be extremely difficult due to the short half-lives of the precursor isotopes.

3 Fabrication of actinide targets

The history of actinide targets dates to the fabrication of a uranium target prepared by precipitation of ammonium diuranate [72] nearly 100 years ago. The fabrication of actinide targets has since had a pivotal role in numerous scientific endeavors, particularly the nucleosynthesis of new nuclides. Today, the variety and complexity of actinide target fabrication techniques has expanded beyond precipitation to include painting [73], vapor deposition [74], sputter coating [75], polymer assisted deposition (with heavy metal surrogates for the actinides) [76, 77], electrodeposition [74], and inkjet printing [78]. The discovery of several new SHEs, including

tennessine (element 117) [9] and oganesson (element 118) [8], involved bombarding actinide targets electrodeposited onto thin metal foils with a high-energy and high-intensity ^{48}Ca beam for several months. The discovery of additional SHEs will require higher beam intensities of several particle microamps and many months of irradiation due to the rapidly decreasing cross sections for the nucleosynthetic pathways of interest [5]. Improvements in separator transmission to around 60% (doubling earlier values of around 30%) and increases in charge particle detection efficiency to about 80% can also contribute to higher rates of observed nuclei [26, 66, 79]. The utilization of thicker targets (up from around 300 $\mu\text{g}/\text{cm}^2$) may also improve sensitivity by covering a larger energy window as suggested by others [79, 80]. Additionally, the mass of projectile nuclei must continue to increase as the mass of actinide targets reaches a maximum due to practical considerations including decreasing material availability and half-lives. Recent efforts to synthesize increasingly heavy nuclides have seen increased actinide target failure rates as more intense and longer-duration irradiations have become necessary. The common failure mode has been thermal degradation of the targets leading to delamination of the actinide films from backing materials as well as pinhole formation. The extreme irradiation conditions required for the next generation of SHE studies will necessitate continued advancements in many technical areas with actinide targets being a key focus.

Electrodeposition has continued as the preferred fabrication technique for producing actinide targets used in nucleosynthesis over the last several decades [81–83]. Electrodeposition results in deposition yields regularly between 90 and 100%. This is very important given the limited availability of many actinide materials. This is especially true for targets made of the rarer actinides, such as berkelium, californium, and einsteinium, for which the maximum amount available at any given time is single to tens of milligrams or far less [5]. Indeed, berkelium and einsteinium rapidly decay relevant to the timescale of nucleosynthesis experiments searching for the heaviest of nuclei. Actinide thin films produced by electrodeposition are also highly reproducible. Target wheel assemblies are required for many SHE studies to dissipate heat loads from the high-current beams through rotation of targets in and out of the beam [84]. Each individual actinide target, often referred to as a segment, must therefore have similar characteristics, such as homogeneity and morphology. Target wheels often consist of more than 10 times the amount of actinide thin film surface area than in the beam at any given time. Electrodeposition is also relatively straightforward to implement in the remote environments often required for handling actinides. Other techniques that require delicate electronics, vacuum chambers, or other complex systems are more difficult to implement remotely,

particularly in environments with radiological contamination controls in place.

The most frequently employed electrodeposition technique is a form of cathodic electrolytic deposition that is performed in a predominately nonconductive, organic solution and commonly referred to in the target community as “molecular plating” [74, 82, 83].

This process involves the deposition of a molecular species in contrast to electrochemical reduction of the actinide to its metallic form (i.e., electroplating). A review of the molecular plating process was recently published by Artes et al. [83]. The electrochemical potentials necessary for reduction of actinides to their metallic forms are outside the potential range of aqueous electrolytes, thereby resulting in the breakdown of water and other molecules. Although the solutions used for molecular plating are mostly nonconductive, organic solutions (e.g., dimethylformamide or isopropanol-isobutanol), they contain a miscible amount of aqueous solution containing a dissolved actinide salt (e.g., metal nitrate or metal chloride). The electrodeposition therefore contains several orders of magnitude more water molecules than actinide ions. The molecular plating process then theoretically proceeds through electroprecipitation of the actinide as a molecular compound (e.g., metal hydroxide or oxide) onto an electrically conductive backing induced by the electrolytic breakdown of water or other molecules at the electrode–solution interface. The electrolytic breakdown of water and other molecules produces hydroxide ions near the electrode–solution interface, thereby dramatically increasing the local pH of the solution. This is hypothesized to result in the electroprecipitation of insoluble actinide hydroxide, which subsequently decomposes to the metal oxide. Other species may also be produced and contained in the final thin film. The exact decomposition pathway is not fully understood and may involve electrochemical and thermal driving forces during the molecular plating process. Postdeposition thermal treatment of actinide targets is often performed to remove residual solvent and likely further decompose remaining actinide hydroxide to the actinide oxide form.

The final properties of electrodeposited actinide thin films depend on factors that include deposition solution composition (e.g., bulk solvent, supporting electrolyte ions, additives); conditions (e.g., temperature, fluid dynamics); and electrical conditions (e.g., pulsed or constant, current density, voltage, cell geometry). Although numerous studies have been performed over the years with actinides and nonradioactive surrogates [83–92], there remains a significant amount of the molecular plating process to explore and understand. Dramatic improvements to the properties of actinide thin film targets prepared through molecular plating could be realized through control of the electrodeposition process enabled by a mechanistic understanding of the deposition process. Further processing after the electrodeposition is completed may

also be used to improve the actinide target characteristics. Thermal treatment of actinide thin films to remove impurities or control evaporation of residual solvent that remains postdeposition is one example. Addition of protective layers through vapor deposition or other techniques is sometimes used to prevent delamination as well as sputtering of actinide material from the target during irradiation.

Actinide thin film targets with improved performance compared to those in use today will likely be required to continue beyond elements 119 and 120. Continued advancement of technologies for thin film deposition and material synthesis is promising for the SHE community. State-of-the-art thin film fabrication techniques afford control of material structures at the microscale and nanoscale [93–95]. Modeling and simulation tools are also increasingly accurate in their prediction of material properties and performance. This unprecedented control can be leveraged to fabricate materials designed to have significantly improved properties for a desired application, such as targets for nucleosynthesis with improved thermal and mechanical properties. Some materials, for example, show strong dependencies of heat transfer and mechanical properties on the orientation of crystallographic planes. Controlled orientation of crystallographic grains within the actinide thin film and/or target backing could improve heat removal and mechanical robustness of actinide targets. Another possibility is the fabrication of alloy or composite materials. Fabrication techniques such as electrodeposition are currently limited to producing actinide oxides on conductive backings. However, electrodeposition methods aside from molecular plating or entirely different fabrication techniques (e.g., inkjet printing) could be developed to produce these types of materials in the future [94].

The materials currently used as backings for actinide targets cannot withstand the irradiation conditions (e.g., doses, particle fluxes) required for future SHE studies. Critical issues are the high thermal loadings and radiation damage. At the same time, current actinide targets benefit from being rotated out of the beam path because there is enough material to build several targets. The development of an actinide target capable of withstanding constant or near-constant irradiation under increasingly intense conditions could enable use of actinide materials with limited availability, such as the transcurium elements californium (certain isotopes), berkelium, and einsteinium. This would likely result in a significant breakthrough for synthesizing new superheavy nuclei. A mechanistic understanding of the processes leading to and causing target failures could enable prediction of ideal target parameters including geometries and compositions, as well as irradiation conditions (e.g., pulse shapes, raster patterns).

Recent SHE target production efforts since 2016 at ORNL have focused on the production of mixed-isotope californium thin films for searches for heavy isotopes of element 118 and new element 120. The californium material, recovered from

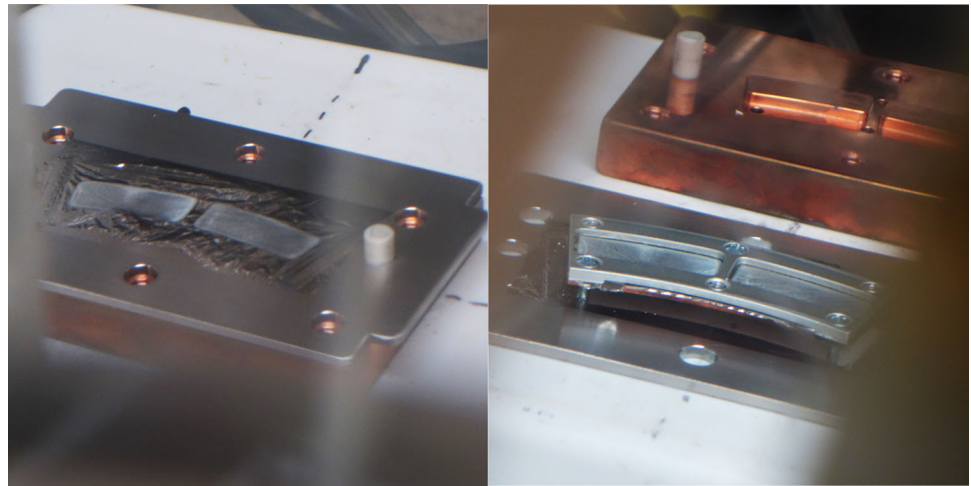
decades old ^{252}Cf targets, is 36% ^{251}Cf , which would be the heaviest isotope to date for SHE experiments. This material also contains significant amounts of ^{249}Cf (48%) and ^{250}Cf (16%). The amounts of ^{250}Cf and ^{252}Cf present in the target can cause material-handling issues due to its intense neutron and gamma radiation. The fabrication of these “mixed-Cf” targets involves a molecular plating process adapted from Vascon et al. [88] and requires the use of a shielded glove box. In 2014, enough mixed-Cf material was recovered and chemically purified to fabricate 12 target segments with roughly 1 mg of mixed-Cf each. These targets were then shipped to JINR for SHE studies. The final target assemblies produced in 2014 were fabricated using a silicone gasket to maintain a liquid-tight seal during electrodeposition. Unfortunately, a film formed on the targets during irradiation, and the experiments had to be halted after an initial observation of a known isotope of element 118 [27] to investigate the source of the film and fabricate new targets. The mixed-Cf material was returned to ORNL and has since been chemically purified. Analysis of the leached target material identified significant quantities of silicone, leading researchers to hypothesize that the silicone gasket may have contributed to the film. The target fabrication process was altered to accommodate removal of the silicone gasket, and the final target assemblies consist of only metal components and the mixed-Cf thin film electrodeposited on the titanium foil backing. The refurbished targets will be used to continue SHE experiments aimed at producing new heavy isotopes of element 118 and new element 120. The electrodeposited targets are shown in Fig. 9.

4 Recent developments in SHE research

Since the last major review in 2015 [96], SHE research has focused on further exploration of the island of stability, including the discovery of new isotopes of known elements and new elements 119 and 120. These studies have depended on actinide targets ^{240}Pu and mixed $^{249-251}\text{Cf}$ at the Flerov Laboratory of Nuclear Reactions (FLNR) at JINR [27] and ^{248}Cm at the Radioactive Ion Beam Facility at RIKEN in Japan [26], and on ^{243}Am for direct mass number measurements of ^{288}Mc and ^{284}Nh isotopes at Berkeley [11]. These actinides were produced/processed at HFIR/REDC through the DOE Isotope Program and Division of Nuclear Physics. Mass measurements based on cold fusion reactions at GSI [36] and RIKEN [37] have been used to determine masses for ^{257}Rf and ^{257}Db , respectively, but the yields are currently too low by several orders of magnitude to determine masses of the heaviest superheavy nuclei.

FLNR and RIKEN use fast data acquisition systems [27, 80, 97, 98] modeled after digital electronics previously developed at ORNL’s Holifield Radioactive Ion Beam Facility for experiments involving short-lived charged particle emitters

Fig. 9 A mixed-Cf thin film electrodeposited onto a titanium foil backing taken through a shielded glove box window (left) before and (right) after final assembly in the metal frame



[99–102]. The ORNL-based system was used at GSI in 2011 during the search for element 120 [103, 104], while GSI-developed digital electronics were used in a confirmation experiment for element 117 [15] and search for elements 119 and 120 [66].

Experiments at JINR with ^{239}Pu and ^{240}Pu targets focused on the identification of new flerovium isotopes produced in the hot fusion reactions with ^{48}Ca beams. Earlier studies using ^{242}Pu and ^{244}Pu target materials with ^{48}Ca beams resulted in the identification of ^{285}Fl to ^{289}Fl in the 3n, 4n, and 5n evaporation channels at JINR [7, 8]; GSI [12, 105]; and Lawrence Berkeley National Laboratory [106]. A long ^{285}Fl decay chain was observed at LBNL in the rare 5n reaction channel of the $^{242}\text{Pu} + ^{48}\text{Ca}$ reaction, but the full energy of the alpha particle emitted by ^{285}Fl was not recorded [10, 106].

A joint US–Russia experiment with a ^{240}Pu target was performed at FLNR with a 245 MeV ^{48}Ca beam, corresponding to an excitation energy of the compound nucleus $^{288}\text{Fl}^*$ between 35.6 MeV and 41.1 MeV [97]. Three decay chains of ^{285}Fl produced in the 3n evaporation channel were identified. The half-life and emitted alpha energy for ^{285}Fl were determined to be $0.15(+0.14, -0.05)$ s and 10.41(5) MeV, respectively. The decay properties of ^{285}Fl daughter activities ^{281}Cn , ^{277}Ds , ^{273}Hs , ^{269}Sg , and ^{265}Rf were measured with higher accuracy [97]. Additional irradiations of the ^{240}Pu target at an increased ^{48}Ca beam energy of 250 MeV did not result in additional ^{285}Fl events, suggesting a 3n cross section below 1.3 fb for 5 MeV higher beam energy (40.9–45.4 MeV excitation for $^{288}\text{Fl}^*$). The four instances of evaporation residue (ER) followed by spontaneous fission (SF) events observed with the 250 MeV beam were assigned to the decay of the new isotope ^{284}Fl . This interpretation was supported by the observation of two similar SF events during the irradiation of a ^{239}Pu target (from RIAR) with ^{48}Ca at 245 MeV selected to maximize the 3n reaction channel, with

35.4 MeV–40.0 MeV excitation energies for the compound nucleus $^{287}\text{Fl}^*$.

Cross sections for Fl isotopes produced in hot fusion reactions with ^{239}Pu , ^{240}Pu , ^{242}Pu , and ^{244}Pu targets and ^{48}Ca beams show dramatic reductions for the most neutron-deficient flerovium isotopes through $^{287}\text{Fl}^*$ compound nucleus, a factor of 50 below the maximum for $^{290}\text{Fl}^*$ and $^{292}\text{Fl}^*$. This indicates that the low-N edge of the Island of Stability in $Z = 114$ isotopes is approximately neutron number $N = 170$ [97].

Because the correlation times between ER and SF signals during the first experiment were scattered, a second experiment with a ^{240}Pu target was performed [98]. With a 250 MeV ^{48}Ca beam, three new events of ^{285}Fl were detected, improving our understanding of the decay properties of all nuclei appearing in this long alpha decay chain that ends with SF of ^{265}Rf . For example, the half-life and alpha energy associated with ^{285}Fl decay are deduced to be $0.10(+0.06, -0.03)$ s and 10.41(5) MeV. The decay of ^{284}Fl was not clarified, and further studies with a higher beam dose are needed for the verification of the origin of detected SF events.

An experiment involving a novel mixed-Cf target was performed at FLNR. The target material, consisting of 51% ^{249}Cf , 13% ^{250}Cf , and 36% ^{251}Cf , was recovered from decayed ^{252}Cf sources at ORNL's REDC and electrodeposited on titanium backing foils. The mixed Cf was irradiated at FLNR with a 252 MeV ^{48}Ca beam, corresponding to an excitation energy of 35.2 ± 2.2 MeV and 36.4 ± 2.2 MeV for the compound nuclei $^{297}\text{Og}^*$ and $^{299}\text{Og}^*$ (calculated for the ^{249}Cf and ^{251}Cf target components), respectively. The search for new isotopes of $Z = 118$ oganesson was the main goal of the investigation. A fifth event of ^{294}Og decay was observed after only 9 days [27]; however, the experiment had to be stopped prematurely due to accumulation of foreign material on the target surface. New target sectors have been electrodeposited at REDC, as discussed in Sect. 3, to

continue the search for new heavy isotopes of oganesson and eventually element 120 (with a ^{50}Ti beam) at the new Super Heavy Element Factory at JINR.

Use of digital electronics has also helped in the analysis of fast fission events detected during the ^{48}Ca + mixed-Cf experiment. Some events had ER–SF correlation times within the range corresponding to the half-life of ^{294}Og , now determined to be 0.58 (+ 44, – 18) ms with the new average decay properties of five known events. The SF decay mode of $Z = 118$ and $N = 176$ ^{294}Og can most likely result in two magic nuclei, ^{208}Pb and ^{86}Kr , which can offer some enhancement of this decay mode. However, no definite conclusion about the origin of fast SF events can be drawn from our data. A setup allowing for some atomic number discrimination such as an ionization chamber in front of the implantation silicon detector may allow future conclusions regarding the properties of implanted nuclei.

Enriched ^{248}Cm material provided by the DOE Isotope Program through ORNL is being used in a joint US–Japan experiment searching for new element 119 at the GARIS-III separator at RIKEN. An intense ^{51}V beam developed at RIKEN and accelerated at the Superconducting RIKEN Linear Accelerator is irradiating a large target wheel with ^{248}Cm sectors electrodeposited at RIKEN. Beam energy was selected by observing elastic and inelastic scattering of heavy ion projectiles on heavy targets including ^{248}Cm [107, 108]. The experiment continues, presently at about 3 particle-microamp beam intensity. This high current is essential to overcome the low-production cross section anticipated for the $^{51}\text{V} + ^{248}\text{Cm}$ reaction (e.g., [44, 45]). Distributing the heat associated with these high beam currents requires larger target areas that necessitate more target material for a given thickness. A summary of current and future superheavy isotope searches is shown in Fig. 10.

5 New and upgraded facilities

Continued progress in SHE research depends on the availability of specialized facilities including high flux reactors and related radiochemical processing facilities for actinide production and high-current heavy ion accelerators including mass separators and related technology for superheavy nucleus synthesis and detection. Production cross sections for superheavy nuclei are declining with increasing Z and N , requiring larger targets and higher current ion beams to support new discoveries. This situation is placing increased demand on actinide supplies and accelerator capabilities. New and upgraded facilities are coming online to meet this challenge.

High flux reactors are key to continued availability of heavy actinides. Currently, these reactors exist only in the United States and Russia—HFIR at ORNL and SM-3 in

Dmitrograd. The PIK Reactor at the Petersburg Nuclear Physics Institute near St. Petersburg, Russia, may also contribute but is not yet operational. HFIR and SM-3 were constructed in the 1960s, and additional investment will be required to guarantee their operation for the long term. A major refurbishment of the SM-3 core was recently completed [109], and planning is under way for life extension and mission upgrades at HFIR [33].

Significant improvements in the production rates for superheavy nuclei at accelerator facilities will also be required, including significant increases in beam currents. The new Superheavy Element Factory [30] at JINR is demonstrating beam currents of 6 particle-microamps and higher for ^{48}Ca , more than six times higher than previously available beams. Upgrades at RIKEN in Japan are also demonstrating multiparticle microamp ion beams [26]. Together with larger targets, a tenfold increase in discovery potential appears to be within reach.

New facilities for superheavy production and research are also in development in France, Germany, and China. At GANIL in France, the NEWGAIN (injector 2) at Spiral2 projects ^{48}Ca beams of 10 particle-microamps and more by 2030 [30]. At GSI in Germany, early components of the Helmholtz Linear Accelerator (HELIAC) [31, 32] are being commissioned. When fully developed, HELIAC offers the potential for an order of magnitude increase in beam intensity compared to UNILAC [31, 32] for new element discovery and related spectroscopy and chemistry studies. The China Facility for Superheavy Elements at the Institute for Modern Physics, Chinese Academy of Sciences (IMP/CAS) together with a new gas-filled separator (SHANS2) are in development for superheavy element studies including synthesis of elements 119 and 120 [110]. In addition, LBNL is developing new capabilities at the 88-inch cyclotron for a proposed search for element 120 using the $^{50}\text{Ti} + ^{249}\text{Cf}$ reaction [28].

5.1 Superheavy element factory

JINR's Superheavy Element Factory [29, 111] was completed in 2020. This facility, shown in Fig. 11, includes a state-of-the-art heavy ion accelerator, experimental hall, facilities for beam transport and superheavy nucleus detection, capabilities for the study of the physical and chemical properties of new elements, and related systems for operations with radioactive materials. The powerful new DC-280 cyclotron has a design beam intensity of up to 10 particle-microamps across a wide range of ion beams including ^{48}Ca . The initial research program will include exploration of the island of stability and searches for new isotopes of element 118 using ^{48}Ca and a search for new element 120 using ^{50}Ti beams with mixed-Cf targets. First experiments with ^{48}Ca on ^{243}Am , ^{242}Pu and ^{238}U targets have been completed [112–114].

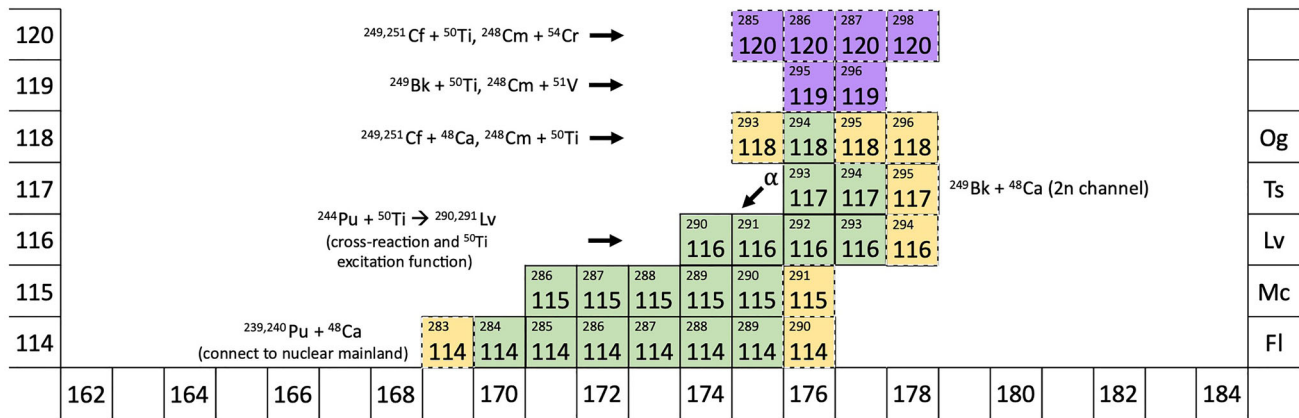


Fig. 10 Current nuclear chart for $Z \geq 114$, including confirmed superheavy isotopes (green), searches under way and planned (purple), and additional superheavy isotopes with a clear path to discovery (yellow). Actinide targets are essential to all of this research



Fig. 11 The new Superheavy Element Factory at JINR in Dubna, Russia

5.2 High Flux Isotope Reactor

HFIR produces the highest steady-state neutron flux in the world, with a peak thermal neutron flux of 2.5×10^{15} neutrons/cm²-s. This peak flux is matched only by the SM-3 Reactor in Dmitrovgrad, Russia. HFIR provides these very high fluxes for growing missions in isotope production, neutron scattering, materials irradiation, neutron activation analysis, and nuclear physics. The Institut Laue Langevin (ILL) Reactor in France, with a peak thermal neutron flux of 1.5×10^{15} neutrons/cm²-sec, is optimized for neutron scattering with limited capability in isotope production. All other research reactors have neutron fluxes lower than HFIR by a factor of 2.5 or more. The very high neutron fluxes of HFIR and SM-3 are essential to enable the multiple neutron captures required for actinide production.

HFIR was constructed in the 1960s to produce measurable quantities of the heavy actinides californium, berkelium, einsteinium, and fermium for research in the new field of Heavy Element Chemistry [115]. The adjacent REDC was constructed at the same time for the processing and purification of highly radioactive materials, including actinides.

The combined capabilities of HFIR and REDC continue to be unique in the world. Figure 12 provides a current photograph of the HFIR/REDC complex.

HFIR has been substantially refurbished over the years. Components that have been replaced/refurbished include primary and backup pumps, the beryllium reflector, beam tubes, heat exchangers, cooling tower, control plates, and electrical and safety systems. The only major system that has not been replaced or refurbished is the pressure vessel. Replacement of the pressure vessel will be required to continue HFIR operation beyond midcentury due to accumulated radiation damage.

HFIR was designed for pressure vessel replacement. Removal of the old vessel and installation of the new vessel can be accomplished using the existing HFIR crane and truck airlock. The vessel can be disconnected and sectioned under water in the existing reactor pool. The vessel is less activated than waste that is routinely disposed at HFIR. Vessel sectioning and replacement has already been demonstrated at the ILL and Petten research reactors in Europe. Figure 13 provides a photo from the original HFIR vessel installation in the mid 1960s.

A new pressure vessel would allow HFIR to return to its original design power level of 100 MWth (from the current operating limit of 85 MWth) with a corresponding 20% increase in neutron flux. It would also allow numerous mission upgrades including improved access for isotope production, improved online insertion/removal of isotope production capsules, and improved facilities for handling irradiated materials. A new vessel would extend HFIR operation into the next century, ensuring continued availability of actinides for research and industrial applications. SM-3 recently completed a major core refurbishment to support continued operation of this reactor beyond 2040 [109].

In 2019, the DOE Office of Science asked its Basic Energy Sciences Advisory Committee to evaluate options for the

Fig. 12 ORNL's research reactor and radiochemical processing complex (HFIR/REDC)

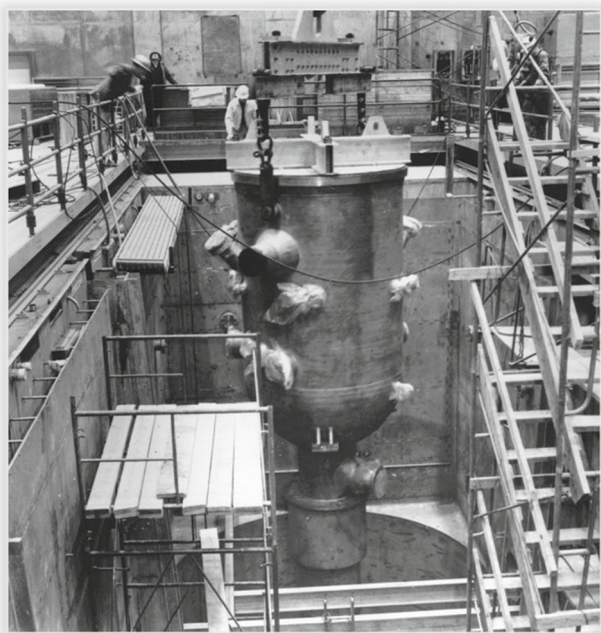


Fig. 13 Original installation of the HFIR pressure vessel

future of HFIR. The committee recommended [33] that DOE immediately pursue the replacement of the reactor pressure vessel to secure the future operation of HFIR and enable increased capability for isotope production, neutron scattering, and other missions. Preliminary planning is under way to accomplish the vessel replacement and related upgrades. At the same time, DOE has directed ORNL to develop plans for expanded radioisotope processing capabilities to support the rapidly growing DOE isotope production and research program.

6 Future opportunities

The past 20 years have seen significant progress in SHE research from nuclear reactions involving actinide targets with intense ^{48}Ca ion beams. Five new elements have been discovered, extending the periodic table to $Z = 118$, and more than 50 new isotopes have been added to the nuclear chart in the vicinity of the island of stability. Lifetimes have been consistent with trends expected from nuclear theory as the shell closure at $N = 184$ is approached. This has been made possible by farsighted investments in high-current accelerators, advanced detectors and mass separators, and actinide production and chemical separation facilities.

Continued progress requires new approaches as production cross sections decline with increasing Z and the limits of ^{48}Ca reactions with available actinides are encountered. Elements 119 and 120 seem accessible, but only with heavier ion beams such as ^{50}Ti , ^{51}V , and ^{54}Cr . Compound nucleus formation using these heavier ions to produce elements 119 and 120 is characterized by lower cross sections by factors of 10 or more [43–45] in comparison to ^{48}Ca reactions for elements 117 and 118. Overcoming these lower cross sections requires increased beam currents and larger and more robust actinide targets. New and upgraded accelerator facilities including the Superheavy Element Factory at JINR and expanded facilities at RIKEN are demonstrating increased ion beam currents of factors of 3 and more. New recovery efforts and production approaches offer the potential of increased availability of key actinides such as ^{248}Cm , ^{249}Bk , $^{249-251}\text{Cf}$, and ^{254}Es . Advances in target technology will also be needed to accommodate the higher thermal loads and increased exposure times of next-generation experiments.

6.1 Exploring the island of stability (Pu, Am, Cm, Bk, and Cf)

Increased beam currents are making 1n and 6n channel experiments with ^{48}Ca beams more attractive, providing potential options for extending the “island of stability” to new lighter and heavier isotopes [112–114]. This will provide additional information on the detailed contours of the island, including the dramatic fall-off in production cross sections for low N isotopes and the effect of the shell closure at $N = 184$ on heavier isotopes. Significant increases in lifetimes are possible, enabling chemistry experiments on some of these new isotopes [38]. These would be primarily ^{48}Ca nuclear reactions with available isotopes of plutonium, americium, curium, berkelium, and californium. As discussed in Sect. 2, many strategies are available for recovering/producing increased amounts of heavy actinide materials for many of these experiments; more than a dozen new isotopes would likely result. For lower N, this could result in decay chains that connect the island to known nuclei on the nuclear mainland, while higher N nuclei will provide additional information on the influence of the shell closure at $N = 184$.

6.2 Discovering elements 119 and 120 (Cm, Bk, and mixed-Cf)

Ongoing and planned experiments to search for elements 119 and 120 have been enabled by increased beam currents at the Superheavy Element Factory at JINR and at RIKEN. These experiments involve nuclear reactions of ^{50}Ti , ^{51}V , and ^{54}Cr beams on ^{248}Cm , ^{249}Bk , and $^{249-251}$ mixed-Cf targets. As discussed in Sect. 2, these heavy actinides can be recovered from legacy ^{252}Cf sources and as a byproduct of current ^{252}Cf production. Availability of ^{249}Bk can also be boosted by dedicated production runs in HFIR using special neutron filters and heavy curium targets. A capability to enrich transuranic actinide isotopes through electromagnetic separators or some other technology would enable production of high-isotopic-purity ^{251}Cf targets, the heaviest target material currently available in sufficient quantities for SHE experiments.

6.3 Electron capture and pxn reactions expanding superheavy island closer to $N = 184$

Moving the existing nuclear chart at the island to higher neutron numbers beyond the reach of present day xn reactions will require new approaches such as pxn reactions followed by electron capture. While pxn channels have previously been observed in cold fusion reactions [116, 117], estimated cross sections for the pxn channels for superheavy nuclei [118–120] are two or more orders of magnitude lower than for current xn reactions in SHE studies. If observed, these

reactions and the resulting decay schemes could push the nuclear chart at the island several additional neutron numbers to the right. These experiments are low probability but could produce new high-N nuclei that are currently unknown.

6.4 Cold fusion path to higher Z and $N = 184$ (mixed-Cf)

Rykaczewski et al. [121] have suggested using a ^{251}Cf target with a ^{58}Fe beam to reach $N = 184$. This would be a cold fusion reaction producing an excited compound nucleus rapidly decaying with one neutron emission to $Z = 124$, $N = 184$ (or to $Z = 124$, $N = 183$ by emitting two neutrons). The excitation energy of the compound nucleus $^{309}(124)^*$ will likely be around 20–25 MeV lower in comparison to the hot fusion reactions, compare chapter 4. Having experimental data on the reactions between actinide targets and beams heavier than ^{48}Ca would help to predict optimum conditions for the search for new element $Z = 124$ near the $N = 184$ neutron number. Although cross sections are expected to be very low (in the femtobarn range [122]), fission barriers should be favorable, and the increased stability at the shell closure may convey additional stabilization [122]. While more theoretical analysis of the expected cross section is needed, the models can be further refined using cross section data following successful searches for element 119 and 120 with beams heavier than ^{48}Ca . An enriched ^{251}Cf target would further increase the probability of success should an actinide separator become available. Reaching the $N = 184$ region would provide unique information on extreme nuclei at the shell closure and verify our current concept of the Island of Stability.

6.5 Future einsteinium options

If available in sufficient quantities, ^{254}Es would be an ideal target to extend reactions using ^{48}Ca beams to $Z = 119$ and reactions using ^{50}Ti beams to $Z = 121$. These reactions should have higher cross sections than the path to $Z = 119$, 121 using Cf targets with ^{50}Ti and ^{54}Cr beams, respectively. While current production of ^{254}Es in HFIR is limited to 1–2 μg , proposed experiments using specialized neutron filters could demonstrate increased production by as much as a factor of 5. This is approaching the scale that would be required to create a small stationary target of the required thickness for SHE discovery experiments. Significant advances in target technology will be required to manage the heat and radiation loads on such a stationary target.

These SHE research opportunities are dependent on the continued availability of heavy actinide targets. Increased attention to actinide production including new production technologies and recovery from existing high-assay sources will be required to ensure sufficient target material for these increasingly challenging experiments. In many cases, these

experiments will also require the development of robust target technologies capable of surviving higher beam currents and heavier ion beams. The continued availability of actinide production and processing facilities such as HFIR and REDC will be essential. There is no apparent substitute for actinide targets as we continue the search for new elements and extreme nuclei with high and low neutron numbers. Expected longer lifetimes at higher N should also enable more sensitive studies of the chemistry of these new elements. Actinide materials have transformed the SHE research field over the past two decades, and the agenda described above offers the potential for decades of progress in the nuclear physics of extreme nuclei and the atomic physics and chemistry of extreme atoms.

Acknowledgements This research was supported by the U.S. Department of Energy (DOE) Office of Isotope R&D and Production and the DOE Office of Nuclear Physics under contract DE-AC05-00OR22725 with UT-Battelle, LLC. We are grateful to the staffs of the ORNL Radiochemical Engineering Development Center and High Flux Isotope Reactor, a DOE Office of Science User Facility, for their support in the production and chemical separation of the actinide materials. We also thank our many collaborators at the Flerov Laboratory of Nuclear Reactions (JINR, Dubna, Russia), GSI (Darmstadt, Germany), University of Mainz (Mainz, Germany), Lawrence Livermore National Laboratory, Vanderbilt University, and the University of Tennessee–Knoxville, without whom this research would not have been possible.

Data availability statement This manuscript has no associated data or the data will not be deposited. [Authors' comment: The focus of this paper is on describing how heavy actinides are used for the synthesis of superheavy nuclei. This paper is not presenting details of those experiments that would have associated data. Nor is this paper presenting details of new processing methods for the supply of actinides. Any such data would be appropriate for inclusion in publications detailing those experiments.]

Open Access This article is licensed under a Creative Commons Attribution 4.0 International License, which permits use, sharing, adaptation, distribution and reproduction in any medium or format, as long as you give appropriate credit to the original author(s) and the source, provide a link to the Creative Commons licence, and indicate if changes were made. The images or other third party material in this article are included in the article's Creative Commons licence, unless indicated otherwise in a credit line to the material. If material is not included in the article's Creative Commons licence and your intended use is not permitted by statutory regulation or exceeds the permitted use, you will need to obtain permission directly from the copyright holder. To view a copy of this licence, visit <http://creativecommons.org/licenses/by/4.0/>.

References

- R. C. Barber, et al., *Pure Appl. Chem.* **83**, 1485 and 1801 (2011). <https://doi.org/10.1351/PAC-REP-10-05-01>
- P.J. Karol et al., *Pure Appl. Chem.* **88**, 139 (2016)
- P.J. Karol et al., *Pure Appl. Chem.* **88**, 155 (2016). <https://doi.org/10.1515/pac-2015-0501>
- Y. Oganessian, *J. Phys. G* **34**, R165 (2007). <https://doi.org/10.1088/0954-3899/34/4/R01>
- J.B. Roberto et al., *Nucl. Phys. A* **944**, 99 (2015). <https://doi.org/10.1016/j.nuclphysa.2015.06.009>
- Yu. Ts. Oganessian et al., *Phys. Rev. C* **69**, 021601(R) (2004). <https://doi.org/10.1103/PhysRevC.69.021601>
- Yu. Ts. Oganessian et al., *Phys. Rev. C* **69**, 054607 (2004). <https://doi.org/10.1103/PhysRevC.69.054607>
- Yu. Ts. Oganessian et al., *Phys. Rev. C* **74**, 044602 (2006). <https://doi.org/10.1103/PhysRevC.74.044602>
- Yu. Ts. Oganessian et al., *Phys. Rev. Lett.* **104**, 142502 (2010). <https://doi.org/10.1103/PhysRevLett.104.142502>
- L. Stavsetra et al., *Phys. Rev. Lett.* **103**, 132502 (2009). <https://doi.org/10.1103/PhysRevLett.103.132502>
- J.M. Gates et al., *Phys. Rev. Lett.* **121**, 222501 (2018)
- Ch.E. Duellmann et al., *Phys. Rev. Lett.* **104**, 252701 (2010). <https://doi.org/10.1103/PhysRevLett.104.252701>
- D. Rudolph et al., *Phys. Rev. Lett.* **111**, 112502 (2013). <https://doi.org/10.1103/PhysRevLett.111.112502>
- S. Hofmann et al., *Eur. Phys. J. A* **48**, 62 (2012). <https://doi.org/10.1140/epja/i2012-12062-1>
- J. Khuyagbaatar et al., *Phys. Rev. Lett.* **112**, 172501 (2014). <https://doi.org/10.1103/PhysRevLett.112.172501>
- Yu. Ts. Oganessian et al., *Phys. Rev. Lett.* **109**, 162501 (2012)
- G.T. Seaborg, *Science* **104**, 379 (1946). <https://doi.org/10.1126/science.104.2704.379>
- G. Münzenberg et al., *Z. Phys. A* **300**, 107 (1981). <https://doi.org/10.1007/BF01412623>
- G. Münzenberg et al., *Z. Phys. A* **309**, 89 (1982). <https://doi.org/10.1007/BF01420157>
- G. Münzenberg et al., *Z. Phys. A* **317**, 235 (1984). <https://doi.org/10.1007/BF01421260>
- S. Hofmann et al., *Z. Phys. A* **350**, 277 (1995). <https://doi.org/10.1007/BF01291181>
- S. Hofmann et al., *Z. Phys. A* **350**, 281 (1995). <https://doi.org/10.1007/BF01291182>
- S. Hofmann et al., *Eur. Phys. J. A* **14**, 147 (2002). <https://doi.org/10.1140/epja/i2001-10119-x>
- K. Morita et al., *J. Phys. Soc. Jpn.* **81**, 103201 (2012). <https://doi.org/10.1143/JPSJ.73.2593>
- Yu. Ts. Oganessian, V. K. Utyonkov, *Nucl. Phys. A* **944**, 62 (2015). <https://doi.org/10.1016/j.nuclphysa.2015.07.003>
- H. Sakai et al., *Eur. Phys. J. A* **58**, 238 (2022)
- N.T. Brewer et al., *Phys. Rev. C* **98**, 024317 (2018). <https://doi.org/10.1103/PhysRevC.98.024317>
- R. Clark, "A US-Led New-Element Search Experiment", 88-Inch Cyclotron DOE Review, Berkeley, CA, March 4–5 (2020). https://urldefense.us/v2?url=https-3A__conferences.lbl.gov_event_301_&d=DwIFaQ&c=v4IIwRuZAmwupIjowmMWUmLasxPEgYsgNI-O7C4ViYc&r=vjmXyXKGbDgCgAjcfSUOoO_20Q-5IrQ334aKR9iHKWU&m=gP3BvKjs2orRtwBGzIjnYXeQht4D_mmI-dutusYhFdcmwIodHNlUxFOK7sB7ri08&s=tZeX8BtmCiYu25w12AGqAFnr5JHmJvYa4UnjXwlXVP0&e=
- A. Karpov, "Superheavy Element Factory". https://indico.in2p3.fr/event/24078/contributions/95500/attachments/64226/88983/Karpov_SHE-Factory.pdf.
- P. Roussel-Chomaz, "GANIL-SPIRAL2 Highlights", ARIS 2023 Conference, Avignon, France. <https://indico.in2p3.fr/event/19688>.
- Ch.E. Duellmann et al., *Radiochim. Acta* **110**, 417 (2022)
- S. Lauber et al., *NIMA* **1040**, 16709 (2022)
- Report of the Basic Energy Sciences Advisory Committee on the scientific justification for a U.S. domestic high-performance reactor-based research facility, US Department of Energy/Office of Science/July 2020. <https://science.energy.gov/bes/community-resources/reports/> DOI: <https://doi.org/10.2172/1647598>
- D. Ackermann, C. Theisen, *Phys. Scripta* **92**, 083002 (2017). <https://doi.org/10.1088/1401-4896/aa7921>

35. O. R. Smits, P. Indelicato, W. Nazarewicz, M. Piibeleht, P. Schwerdtfeger, Pushing the Limits of the Periodic Table – A Review on Atomic Relativistic Electronic Structure Theory and Calculations for the Superheavy Elements, arXiv 2301.02553 (2023), submitted to Phys. Reports.
36. O. Kaleja et al., Phys. Rev. C **106**, 054325 (2022)
37. P. Schury et al., Phys. Rev. C **104**, L021303 (2021)
38. A. Turler and V. Pershina, Chem. Rev. **113**, 1237 (2013).
39. S.M. Robinson et al., Radiochim. Acta **108**(9), 737–746 (2020). <https://doi.org/10.1515/ract-2020-0008>
40. Hogle, Susan, "Optimization of Transcurium Isotope Production in the High Flux Isotope Reactor." PhD diss., University of Tennessee, 2012. https://trace.tennessee.edu/utk_graddiss/1529
41. S. Hogle, G.I. Maldonado, C. Alexander, Ann. Nucl. Energy **60**, 267 (2013) <https://doi.org/10.1016/j.anucene.2013.05.018>
42. Yu. Ts. Oganessian et al., Phys. Rev. C **62**, 041604(R) (2000). <https://doi.org/10.1103/PhysRevC.62.041604>
43. G. Adamian et al., Phys. Particles and Nuclei **47**, 387 (2016)
44. K. Siwek-Wilczyńska, T. Cap, M. Kowal, Phys. Rev. C **99**, 054603 (2019). <https://doi.org/10.1103/PhysRevC.99.054603>
45. G. G. Adamian and N. V. Antonenko, Eur. Phys. J. A **58**, 111 (2022). <https://doi.org/10.1140/epja/s10050-022-00764-0>
46. Ch. E. Duellmann et al., J. Radioanal. Nucl. Chem. **332**, 1505 (2023)
47. 2019 Heavy Element Chemistry Principal Investigators' Meeting, Gaithersburg, MD, April 15–17 (2019). https://science.osti.gov/-media/bes/csgb/pdf/docs/2019/HEC_Proceedings_2019.pdf. Accessed 29, July, 2022
48. K.P. Carter et al., Nature **590**, 85–88 (2021). <https://doi.org/10.1038/s41586-020-03179-3>
49. I. W. Osborne-Lee, C. W. Alexander, Oak Ridge National Laboratory Technical Report, ORNL/TM–12706 (1995). <https://doi.org/10.2172/205871>
50. R. G. Haire, in The Chemistry of the Actinide and Transactinide Elements 4th edn Vol 3. (Springer 2011), p. 1499
51. J.E. Bigelow, et al, in *Actinide Separations ACS Symposium Series*, vol. 117, ed. by J.D. Navratil, W.W. Schulz (American Chemical Society, Washington, DC, 1980), pp.161–171
52. E.D. Collins, et al, in *Transplutonium Elements-Production and Recovery ACS Symposium Series*, vol. 161, ed. by J.D. Navratil, W.W. Schulz (American Chemical Society, Washington, DC, 1981), pp.147–160
53. E.K. Hulet et al., J. Inorg. Nucl. Chem. **17**, 350–360 (1961). [https://doi.org/10.1016/0022-1902\(61\)80161-9](https://doi.org/10.1016/0022-1902(61)80161-9)
54. D.E. Benker, et al, in *Transplutonium Elements-Production and Recovery ACS Symposium Series*, vol. 161, ed. by J.D. Navratil, W.W. Schulz (American Chemical Society, Washington, DC, 1981), pp.161–172
55. G.R. Choppin et al., J. Inorg. Nucl. Chem. **2**, 66–68 (1956). [https://doi.org/10.1016/0022-1902\(56\)80105-X](https://doi.org/10.1016/0022-1902(56)80105-X)
56. W. Bickford, Westinghouse Savannah River Company Report, OBU-OPD-2003–00043 (2003)
57. B. D. Patton, et al., Special Actinide Recovery from Mark-18A Target Material. United States. (2017)
58. S. M. Robinson et al., Oak Ridge National Laboratory Technical Report, ORNL/TM-2014/314 (2014)
59. A. Sobiczewski, F.A. Gareev, B.N. Kalinkin, Phys. Rev. Lett. **22**, 500 (1966)
60. W.D. Myers, W.J. Swiatecki, Nucl. Phys. **81**, 1 (1966)
61. A. Sobiczewski, K. Pomorski, Prog. Part. Nucl. Phys. **58**, 292 (2007)
62. S. Cwiok, P.-H. Heenen, W. Nazarewicz, Nature (London) **433**, 705 (2005)
63. Yu. Ts. Oganessian, J. Phys. G: Nucl. Part. Phys. **R165** (2007)
64. S. Hofmann et al., Eur. Phys. J. A **52**, 180 (2016). <https://doi.org/10.1140/epja/i2016-16180-4>
65. Yu. Ts. Oganessian et al., PRC **79**, 024603 (2009).
66. J. Khuyagbaatar et al., Phys. Rev. C **102**, 064602 (2020)
67. L. K. Felker, L. H. Delmau, "Recovery of ²⁴⁸Cm from ²⁵²Cf decay," in The 8th International Conference on Isotopes Proceedings (American Nuclear Society 2014)
68. Boll, Rose Ann. Californium Electrodepositions at Oak Ridge National Laboratory. United States. <https://doi.org/10.1007/s10967-015-4148-8>
69. M. Du, et al., Oak Ridge National Laboratory Technical Report, ORNL/TM- 2019/1138 (2019).
70. M. Schaedel et al., PRC **33**, 1547 (1986)
71. K. Nishio et al., "Competition between mass-symmetric and asymmetric fission modes in ²⁵⁸Md produced in the ⁴He + ²⁵⁴Es reaction", submitted to Phys. Rev. Lett. (2023), and private communication 2023.
72. G. Herrmann, Nucl. Instrum. Methods A **282**, 301 (1989). [https://doi.org/10.1016/0168-9002\(89\)90157-5](https://doi.org/10.1016/0168-9002(89)90157-5)
73. L.V. Drapchinsky et al., Nucl. Instrum. Methods Phys. Res. A **438**, 116 (1999). [https://doi.org/10.1016/S0168-9002\(99\)00948-1](https://doi.org/10.1016/S0168-9002(99)00948-1)
74. K.M. Glover, Nucl. Instrum. Methods Phys. Res. A **236**, 435 (1985). [https://doi.org/10.1016/0168-9002\(85\)90939-8](https://doi.org/10.1016/0168-9002(85)90939-8)
75. J. Kwinta, Nucl. Instrum. Methods **167**, 65 (1979). [https://doi.org/10.1016/0029-554X\(79\)90478-6](https://doi.org/10.1016/0029-554X(79)90478-6)
76. M.A. Garcia et al., Thin Solid Films **516**, 6261 (2008). <https://doi.org/10.1016/j.tsf.2007.11.127>
77. M.A. Garcia et al., Nucl. Instrum. Methods Phys. Res. A **613**, 396 (2010). <https://doi.org/10.1016/j.nima.2009.09.084>
78. R. Haas et al., Nucl. Instrum. Methods Phys. Res. A **874**, 43 (2017). <https://doi.org/10.1016/j.nima.2017.08.027>
79. Yu. Ts. Oganessian et al., Nucl. Instr. Meth A **1033**, 166640 (2022)
80. P. Brionnet et al., Nucl. Instr. Meth A **1049**, 168068 (2023). <https://doi.org/10.1016/j.nima.2023.168068>
81. J.D. Burns et al., Nucl. Instrum. Methods Phys. Res. A **830**, 95–101 (2016). <https://doi.org/10.1016/j.nima.2016.05.062>
82. W. Parker, R. Falk, Nucl. Instrum. Meth. **16**, 355–357 (1962). [https://doi.org/10.1016/0029-554X\(62\)90142-8](https://doi.org/10.1016/0029-554X(62)90142-8)
83. E. Artes et al., EPJ Web of Conferences **285**, 03001 (2023). <https://doi.org/10.1051/epjconf/202328503001>
84. S. Antalic et al., Nucl. Instrum. Methods Phys. Res. A **530**, 185–193 (2004). <https://doi.org/10.1016/j.nima.2004.04.217>
85. J. Runke et al., J. Radioanal. Nucl. Chem. **299**, 1081–1084 (2014). <https://doi.org/10.1007/s10967-013-2616-6>
86. A. Vascon. Molecular plating of thin lanthanide layers with improved material properties for nuclear applications. Ph.D. Thesis, Johannes Gutenberg-Universität (2013). Available from INIS: http://inis.iaea.org/search/search.aspx?orig_q=RN:46021465
87. A. Vascon et al., J. Radioanal. Nucl. Chem. **299**(2), 1085–1091 (2014). <https://doi.org/10.1007/s10967-013-2631-7>
88. A. Vascon et al., Nucl. Instrum. Meth. A **721**, 35–44 (2013). <https://doi.org/10.1016/j.nima.2013.04.050>
89. K. Myhre et al., Surf. Sci. Spectra **23**, 70 (2016). <https://doi.org/10.1116/1.4954390>
90. M.N. Torrico et al., Nucl. Instrum. Meth. A **790**, 64–69 (2015). <https://doi.org/10.1016/j.nima.2015.03.056>
91. K.G. Myhre et al., Surf. Sci. Spectra **25**, 024003 (2018). <https://doi.org/10.1116/1.5052011>
92. R.A. Boll et al., J. Radioanal. Nucl. Chem. **305**(3), 921–926 (2015). <https://doi.org/10.1007/s10967-015-4148-8>
93. O.O. Abegunde et al., AIMS Mater. Sci. **6**(2), 174–199 (2019). <https://doi.org/10.3934/matserci.2019.2.174>
94. C. Androulidakis, et al., 2D Mater. **5**(3), 032005 (2018). <https://doi.org/10.1088/2053-1583/aac764>
95. Z. Aksamija, ECS Meet. Abstr. MA2020–01(50), 2767 (2020). <http://https://doi.org/10.1149/MA2020-01502767mtgabs>

96. Special Issue on Superheavy Elements, Nucl. Phys. A 944 (2015), edited by Ch. E. Duellmann, R.-D. Herzberg, W. Nazarewicz, and Y. Oganessian
97. V.K. Utyonkov et al., Phys. Rev. C **92**, 034609 (2015). <https://doi.org/10.1103/PhysRevC.92.034609>
98. V.K. Utyonkov et al., Phys. Rev. C **97**, 014320 (2018). <https://doi.org/10.1103/PhysRevC.97.014320>
99. K. Rykaczewski et al., Nucl. Phys. A **701**, 179 (2002). [https://doi.org/10.1016/S0375-9474\(01\)01569-X](https://doi.org/10.1016/S0375-9474(01)01569-X)
100. R. Grzywacz, Nucl. Instrum. Meth. B **204**, 649 (2003). [https://doi.org/10.1016/S0168-583X\(02\)02146-8](https://doi.org/10.1016/S0168-583X(02)02146-8)
101. R. Grzywacz et al., Nucl. Instrum. Meth. B **261**, 1103 (2007). <https://doi.org/10.1016/j.nimb.2007.04.234>
102. I.G. Darby et al., Phys. Rev. Lett. **105**, 162502 (2010). <https://doi.org/10.1103/PhysRevLett.105.162502>
103. D. Miller, et al., GSI Scientific Report 2011, (GSI Report 2012–1, pp 220, 2012). <http://www.gsi.de/library/GSI-Report-2012-1/>
104. S. Hofmann, S. Heinz, R. Mann et al., Review of even element super-heavy nuclei and search for element 120. Eur. Phys. J. A **52**, 180 (2016). <https://doi.org/10.1140/epja/i2016-16180-4>
105. J.M. Gates et al., Phys. Rev. C **83**, 054618 (2011). <https://doi.org/10.1103/PhysRevC.83.054618>
106. P.A. Ellison et al., Phys. Rev. Lett. **105**, 182701 (2010). <https://doi.org/10.1103/PhysRevLett.105.182701>
107. T. Tanaka et al., Phys. Rev. Lett. **124**, 052502 (2020). <https://doi.org/10.1103/PhysRevLett.124.052502>
108. M. Tanaka et al., J. Phys. Soc. Jpn. **91**, 084201 (2022). <https://doi.org/10.7566/JPSJ.91.084201>
109. A. A. Tuzov, et al., SM-3 Core Refurbishment Project. (International Group on Research Reactors, 2021), <https://www.igorr.com/Documents/2021/07.1%20TM-%20RIAR-SM-3%20CORE%20REFURBISHMENT%20PROJECT.pdf>. Accessed 29 July 2022
110. Z.G. Gan et al., Eur. Phys. J. A **58**, 158 (2022)
111. S. Dmitriev, et al., EPJ Web Conf. 131, 08001 (2016), Nobel Symposium NS160 – Chemistry and Physics of Heavy and Superheavy Elements. <https://doi.org/10.1051/epjconf/201613108001>
112. Yu. Ts. Oganessian et al., Phys. Rev. C **106**, L031301 (2022)
113. Yu. Ts. Oganessian et al., Phys. Rev. C **106**, 064306 (2022)
114. Yu. Ts. Oganessian et al., Phys. Rev. C **106**, 024612 (2022)
115. A. Weinberg, Phys. Today **20**(6), 23 (1967). <https://doi.org/10.1063/1.3034353>
116. A. Lopez-Martens et al., Phys. Lett. B **795**, 271 (2019)
117. F.P. Hessberger et al., Eur. J. Phys. A **55**, 208 (2019)
118. J. Hong et al., Phys. Lett. B **809**, 135760 (2020). <https://doi.org/10.1016/j.physletb.2020.135760>
119. J. Hong et al., Phys. Rev. C **103**, L041601 (2021). <https://doi.org/10.1103/PhysRevC.103.L041601>
120. J. Hong et al., Phys. Lett. B **805**, 135438 (2020). <https://doi.org/10.1016/j.physletb.2020.135438>
121. K.P. Rykaczewski et al., EPI Web Conf. **131**, 05005 (2016). <https://doi.org/10.1051/epjconf/201613105005>
122. K. Wilczynska, private comm. (2016)